Journal of the Medical Research Institute

JMRI, 2025; Vol. 46 No.3: (23-31)

Journal of the Medical Research Institute

Study some biophysical properties of baker's yeast Saccharomyces cerevisiae as a potential nutritional source to address food issues related to animal protein.

Rasha Said ShamsElDine Moust[1]*, Moustafa Hussein Moustafa[1]

1) Medical Biophysics Department,Medical Research Institute, Alexandria University, Egypt.

ABSTRACT:

To address the growing challenge of limited access to adequate nutrition, global initiatives have focused on identifying alternative, cost-effective, and environmentally sustainable protein sources. Among these, yeast-derived proteins have gained increasing attention in the food industry due to their high content of essential amino acids, including lysine, methionine, and phenylalanine. Yeast proteins consist of amino acids, which may exist in zwitterionic forms. These forms exhibit dipole-like behavior, influencing their interactions with solvents and other biomolecules, which is particularly relevant for pharmaceutical applications and protein formulation. Despite this potential, the electrical properties of yeast proteins remain. have not been systematically studied. In this study, we investigate the electrical characteristics of proteins extracted from baker's yeast (*Saccharomyces cerevisiae*). Complex impedance spectroscopy was employed to examine the frequency-dependent dielectric constant and loss factor at ambient temperature (~298 K) over a frequency range of 1 kHz to 1 MHz. The AC conductivity of the samples was found to follow Jonscher's universal power law, indicating the coexistence of multiple transport mechanisms. Analysis of Nyquist and Cole–Cole plots revealed semicircular arcs, while complex electric modulus analysis indicated non-Debye type relaxation behavior. The stretching exponential factor (β) was determined by fitting the modified Kohlrausch–Williams–Watts (KWW) equation to the imaginary component of the electric modulus.

Keywords: yeast protein, impedance, dielectric, loss factor, spectroscopy.

1. INTRODUCTION

The global population is significantly affected by limited access to food. Approximately 735 million people suffer from food insecurity, hunger, and malnutrition. More than 3 billion people cannot afford a healthy, balanced diet (*Ibarra ,2021, Olagunju, 2023*). These challenges have led to increased consumption of energy-dense, nutrient-poor foods, contributing to a rise in chronic health conditions such as obesity, cardiovascular diseases, and type 2 diabetes (*Ziso et al, 2023*).

Proteins are among the most widely consumed macronutrients globally. Yeasts, such as *Saccharomyces cerevisiae*(S.c.Y), *Kluyveromycesmarxianus*, and *Candida utilis*, are single-celled eukaryotic microorganisms recognized for their potential as alternative protein sources. These yeasts are considered Generally Recognized as Safe (GRAS) by the U.S. Food and Drug administration. They can be cultivated on various low-cost and sustainable substrates, including lignocellulosic sugars and waste lactose, making them an environmentally friendly option for protein production. Incorporating yeast-derived proteins into diets could play a pivotal role in addressing global protein demands while promoting sustainability *(Mirzaei, M et al, 2018)* .Yeast is a group of single-celled eukaryotic microorganisms, comprised of strains such asSaccharomyces cerevisiae, Kluyveromycesmarxianus, and Candida utilis, all recognized as consumption-generally recognized as safe (GRAS) by the US Food and Drug Administration. Compared to animal and plant proteins, yeast proteins have been reported to be more sustainable, nearly allergen-free, cleaner, and more economical (*Dimopoulos, G., et al,2021*)

Saccharomyces cerevisiae is the strain used in over 90% of yeast-based products. It is inoculated into a nutrient-rich fermenter (such as one containing molasses) and cultured through fermentation. The supernatant component of the enzymatic hydrolysis is used to make yeast extract for use as food seasoning *(Stam, J.C., et al,1998).* Recently, the European Food Safety Authority (EFSA) approved the use of proteins from *Yarrowi alipolytica* yeast, cultured in waste substrates, as dietary supplements for individuals over 3years

Corresponding author: **Rasha Said ShamsElDine Moust** Received: 26-8-2025 Accepted: 24-9-2025

of age, affirming that yeast proteins are safe and nutritious (*Jach, 2022*). Protein constitutes 35–60% of yeast dry weight and boasts a well-balanced amino acid profile (*Ma et.al,2023)*

The precipitation, which contains most of the proteins, is used to make yeast protein (YP). YP content is upwards 70% and it contains all the essential amino acids required by the human body–In addition, YP contains trace minerals and B-vitamins. Compared with bean protein. Thus, yeast protein holds significant potential as a source of high-quality protein for human consumption (*Ma et.al,2023)*.

The study of the dielectric properties of the yeast *Saccharomyces cerevisiae* is important and useful for cancer research. Insights into cell dielectric behavior from yeast can support technologies that distinguish cancerous cells from healthy ones using electric field responses (*Gascoyne et al,2002)* drug efficacy testing, since the changes in dielectric properties after antifungal exposure can indicate drug efficacy and cellular response (*Ruan et al,2013*) electroporation and drug delivery because the dielectric properties are critical for optimizing electroporation conditions for gene delivery in yeast, which informs mammalian cell applications (*Kotnik, T., et al, 2015)*, and finally, as model System for Human Cells for understanding membrane properties and apoptosis, which are relevant to human diseases *(Gascoyne et al, 2002)*.

Protein amino acids can exist in an ionic form known as zwitterions, as illustrated in Figure 1. These molecules possess both cationic and anionic characteristics, with a distinctive charge distribution that enables interaction with electric fields. This interaction gives rise to notable dielectric properties, allowing favorable interactions with both polar and nonpolar environments. The dipole polarization of zwitterions helps explain how these molecules respond to external electric fields *(Ozols, 1990*)

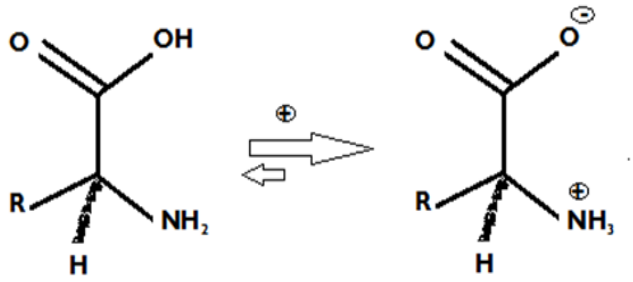

Figure 1: the schematic illustration of zwitterions and its ionizing states

These parameters offer valuable insights into the interactions of amino acids with solvents and other biomolecules, influencing pharmaceutical design and the development of advanced biomaterials. Furthermore, the dielectric properties and loss factors of amino acids are influenced by their purity and ionization states, which play a critical role in shaping their overall dielectric behavior (*Anthony et al, 1*989).

When alternating electrical current flows through biological tissues, it travels through both extracellular and intracellular fluids, depending on the current's frequency and the electrical properties of the different tissues (*Kao , 2004).*

Conductivity refers to the amount of current that will flow through tissues when an electric field is applied. Permittivity measures the charge induced and stored at tissue interfaces (such as membranes) by the electric field. Resistivity is the inverse of conductivity. These parameters of interacting tissues are typically linear, isotropic, and time independent (*Asami, 1976*).

The electrical behavior of biological tissues is often compared to electrical circuit models resistor-capacitor circuit (RC) Figure 2. The simplest and most used model is called "Randles cell". This model represents the extracellular pathway of current by a single resistor (Re) parallel with the resistance of intracellular fluid (Ri) and a capacitor (C) representing the enclosing cell membranes as in Figure 2. The impedance (Z) of this equivalent circuit at a specific angular frequency (ω) (where $\omega = 2\pi f$) is given by

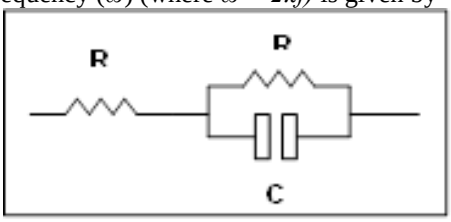

Figure 2: *Randle* cell model of biological tissues.

Loss tangent or the dissipation factor $\tan\delta$, is a measure of energy lost in a dielectric material due to charge carrier or dipolar polarization. It is the ratio of the imaginary part to the real part of the complex permittivity of the material (*Asami, 1976*). Mathematically, it is expressed as part of the complex permittivity of the material. as in $\tan\delta = \frac{\varepsilon'}{\varepsilon''}$

$$\tan\delta = \frac{\varepsilon_r}{\varepsilon_i} \qquad \textbf{Equation 1}$$

The Nyquist plot serves as a parametric representation utilized for the assessment of the stability of a dynamic system or transfer function. This plot was conceptualized by the Swedish American electrical engineer Harry Nyquist at Bell Telephone Laboratories in the year 1932. A method for relating the dielectric response of real materials with assumed Debye behavior was developed by K. S. Cole and R. H. Cole in. He introduced the so-called Cole–Cole plot as mentioned in Randles model Figure 2 *(Kiani et al, 2020)*

Cole suggested that in this case the complex dielectric constant might follow the empirical relation originates from the basic Debye model that presents a normalized form of complex permittivity(ε_ω) based on a single average relaxation time (τd) as shown in Equation **2**

$$\frac{\varepsilon_{\omega}-\varepsilon_{\infty}}{\varepsilon_0-\varepsilon_{\infty}} = \frac{1}{1+j\omega\tau_d} \qquad \textbf{Equation 2}$$

Where $\omega = 2\pi$ f is the angular frequency, ε_0 is the static dielectric constant, and ε_∞ is the dielectric constant at infinite frequency.

The aim of this study

The main goal of this study to test whether impedance spectroscopy can characterize yeast proteins as functional biomaterials, and possibly relate their electrical properties to food or biomedical applications, also to investigate the dielectric impedance of yeast-extracted protein as a potential food protein source for subsequent food-biotechnology applications

Material and methods

This study adopted an experimental quantitative research design, wherein the effects of the independent variables, frequency and temperature on the dependent variable(s) were systematically examined. This approach allows for precise measurement and control of variables, facilitating a clear understanding of causal relationships.

The impedance data from Nyquist and Cole-Cole plots were analyzed using Zsimpwin 7.0 software to determine the equivalent circuit model and to describe the electrical response of the system, and then separated into their real and imaginary components, which were subsequently used to calculate the dielectric constant, dielectric loss, and complex conductivity.

Preparation for Yeast Cell Suspension

The preparation method for yeast cells suspension was adopted from the work of *Vanderwaeren et al (2022)* , Dry baker's yeast was sourced from a local bakery in Alexandria, Egypt. To prepare the yeast suspension, 10 g of dry yeast was dissolved in 100 mL of Base Solution (BS) and stirred for 5 minutes using a magnetic stirrer, yielding a suspension with an approximate concentration of 10^9 CFU/mL. The BS comprised 20 mM KH_2PO_4, 30 mM KCl, and 1 mM $MgCl_2$, adjusted to pH 6.5.

Subsequently, 65 mL of this suspension was centrifuged at 5000 rpm for 10 minutes. The resulting pellet was resuspended in 65 mL of fresh BS and stirred magnetically. This washing procedure was repeated five times to ensure the thorough removal of biological debris. The conductivity of the final washed yeast suspension was measured and found to match that of the BS, at 5.47 ± 0.06 mS/cm.Figure 3(1,2,3)

Trichloroacetic Acid (TCA)/Acetone Protein Extraction

The TCA/acetone method enables selective protein precipitation while effectively removing lipids and carbohydrates that could interfere with downstream applications such as mass spectrophotometry. Additionally, this technique helps preserve protein structure and function, allowing researchers to analyze proteins in their native state an essential aspect for understanding biochemical pathways and interactions within yeast cells *(Vanderwaeren,2022; Natalino Natalino,2023)*.

Most proteins precipitate at low pH and subsequently re-dissolve when the pH increases. A 10% solution of TCA (pH ≈ 1.2) is added to the yeast protein suspension while stirring mechanically at a controlled low temperature (4°C). This process disrupts hydrogen bonding interactions that stabilize proteins in solution, causing them to become insoluble and enable the pelleting of cellular debris along with the precipitated proteins. The acidic environment created by TCA also inactivates proteolytic enzymes, thereby minimizing protein degradation. Proteins are insoluble in acetone (25 mM) and rapidly precipitate at low temperatures, while various buffer contaminants remain soluble. This allows for the isolation of extracted yeast whole protein (EYP) precipitate, which can then be dried and stored for future use *(Vanderwaeren, 2022; Natalino Natalino,2023)*

The optical properties of protein amino acids provide valuable insights not only into their electronic structure but also into protein dynamics and interactions. Interactions between charged side chains can result in unique charge transfer processes, enhancing our understanding of how these biomolecules respond to external stimuli such as changes in temperature and pH. The ultraviolet (UV) spectrum of YEP was analyzed by measuring the absorbance in the UV-visible region (200–900 nm) using a JENWAY 6305

Complex impedance measurement

Before measurement, the YEP sample was compressed into a circular pellet. The pellet was placed in a circular cuvette with a radius of 5 mm and a length of 10 mm. The measuring electrodes consisted of a pair of parallel silver plates positioned on opposite sides of the cuvette, as shown in figure 3

Impedance (Z), phase angle (θ), capacitance (C), and tan(δ) were measured over a frequency range of 1 kHz to 1 MHz using an LCR meter (Fluke PM 6306) at room temperature (~298 K). Four-terminal Kelvin clips were employed along with a shielding design to minimize electromagnetic interference noise during the measurements.

From the data, we calculated the real (z') and imaginary (z") parts of the complex impedance (Z*) by the equations **Error! Not a valid bookmark self-reference.**:

$$z'_{\omega} = \mathbf{Z}^{*}.\cos(\boldsymbol{\theta}) \qquad \textbf{Equation 3}$$

$$z"_{\omega} = \boldsymbol{Z}^{*}.\sin(\boldsymbol{\theta}) \qquad \textbf{Equation 4}$$

Where: $Z = z' - jz"\ \ , j = \sqrt{-1}$

The dielectric constant's real (ε'') and imaginary (ε'') parts can be calculated using the

$$\boldsymbol{\varepsilon'_{\omega}} = \boldsymbol{C_m}.\frac{\boldsymbol{d}}{\boldsymbol{\varepsilon_o}.\boldsymbol{A}} \qquad \textbf{Equation 5}$$

$$\boldsymbol{\varepsilon"_{\omega}} = \boldsymbol{\varepsilon_r}.\tan\boldsymbol{\delta} \qquad \textbf{Equation 6}$$

Where C_m is measured capacitance, d is the sample thickness, ε_o is the permittivity of free space, and A is the cross sectional area of electrode surface .

To predict the conduction mechanism of the present sample, the ac conductivity has been calculated from dielectric data using the formula in Equation **7**:

$$\boldsymbol{\sigma_{ac}} = \boldsymbol{\varepsilon_r\varepsilon_0\omega}\tan\boldsymbol{\delta} \qquad \textbf{Equation 7}$$

Where $\omega=2\pi f$

The Jonscher power model was performed to fit the conductivity data by using equation 8 to explain its behavior.

$$\boldsymbol{\sigma_{ac}} = \boldsymbol{\sigma_{dc}} + \boldsymbol{A\omega^{S}} \qquad \textbf{Equation 8}$$

Where (σ ac) is the total conductivity, (σdc) is the dc conductivity, (A) is the temperature-dependent parameter having a unit of conductivity and it determines the strength of the polarizability. (s) is the frequency exponent whose value lies between 0 and 1 and s is the frequency exponent.

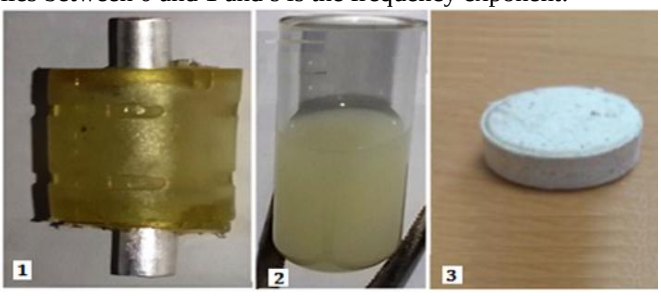

Figure 3 photograph showing dielectric measurer cell **(1)**, yield ,**(2)**YEPand **(3)**compressed pellet

Nyquist and Cole-Cole plots

The impedance data from Nyquist and Cole-Cole plots were fitted using Zsimpwin 7.0 software to identify the equivalent circuit model and characterize the electrical response of the system. The impedance data were then decomposed into their real and imaginary components, which were further converted into dielectric constant, dielectric loss, and complex conductivity values.

Statistical Analysis:

All experimental data were analyzed and presented as the mean ± standard deviation ($n \geq 3$). Origin 8.0 (OriginLab, Northampton, MA, USA) and SPSS 16.0 (SPSS Inc., Chicago, IL, USA) were used to analyze differences among datasets and to generate graphical illustrations. Descriptive statistics were calculated and reported appropriately. Parametric tests for normality were conducted with a 95% confidence interval.

Results

Complex Impedance Analysis

Figure 4 illustrates the UV-visible spectrum optical absorbance of EYP

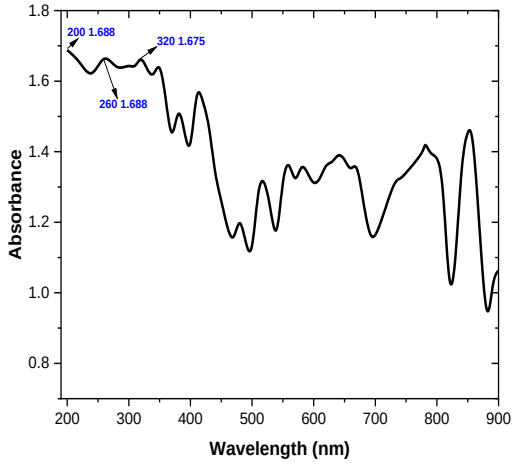

Figure 4 : UV-visible spectrum optical absorbance of EYP

The UV-visible absorbance spectrum of yeast proteins is characterized by distinct peaks corresponding to specific molecular components:

Aromatic Amino Acids: Proteins inherently absorb UV light at 280 nm due to the presence of aromatic amino acids like tryptophan and tyrosine. Nucleic Acids absorb UV light at 260 nm, and cellular Components with the absorbance peaks at 310, 350, 400, and 427 nm in yeast cells. These peaks are attributed to various cellular components and their interactions.

Root mean square error of the absolute relative permittivity (ε) and impedance (Z) for yeast protein powder (EYP) against frequency are shown in figure 5

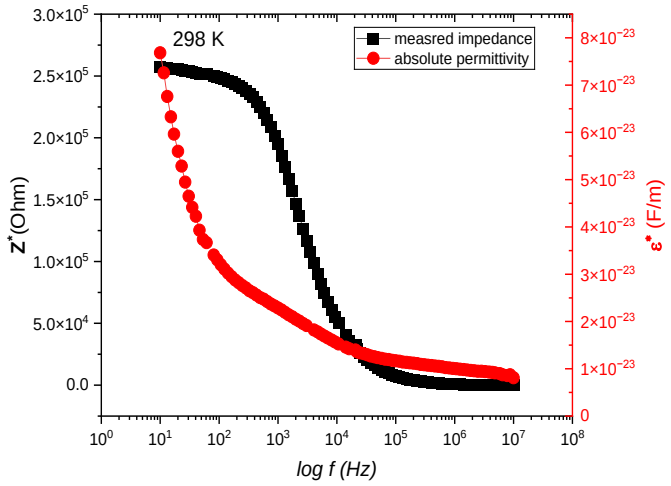

Figure **5** frequency variation for absolute impedance (left) and dielectric permittivity (right) at working temperature

The exploration of the frequency dependence regarding both the dielectric constant ε' and the dielectric loss ε" displayed in figure 6 reveals a significant decline in both parameters with frequency, which may denote the conventional behavior of dielectric materials.

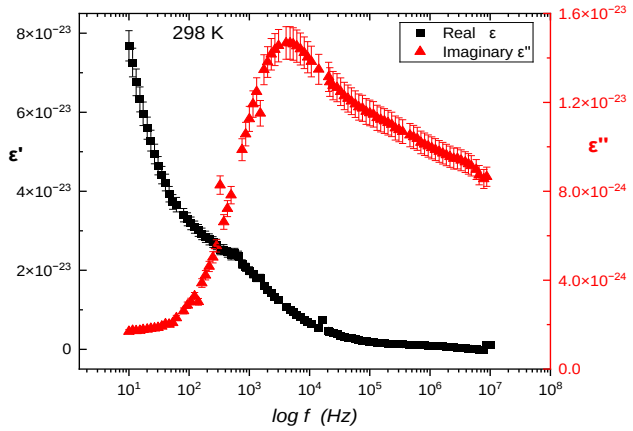

Figure 6: Complex dielectric components variation with applied frequency at 298 K

The cell suspensions behave differently than bulk dielectrics. At low frequencies, the cell membrane acts like an insulator, and the polarization of dipoles inside the cell is limited. Accordingly, the yeast cells do not effectively store electric field energy, leading to a low dielectric constant, because their membranes block dipole alignment. The restricted movement of charges or dipoles in and around the cells results in low energy storage at low frequencies.

The imaginary part of permittivity (ε'') is often called dielectric loss is related to energy loss or dissipation. At low frequency, mobile ions accumulate at the membrane interface (due to the presence of the insulating cell membrane). This is known as Maxwell–Wagner interfacial polarization. This

accumulation leads to high ionic conduction losses, which increases ε″.

The yeast cells dissipate a lot of electrical energy as heat due to ionic conduction and interfacial polarization at low frequencies.

Complex impedance analysis

Dielectric loss tangent (tanδ) with quality factor (Q) trend with frequency the working temperature for the sample is plotted in Figure 5. The dielectric loss shows a decrease with an increase in frequency.

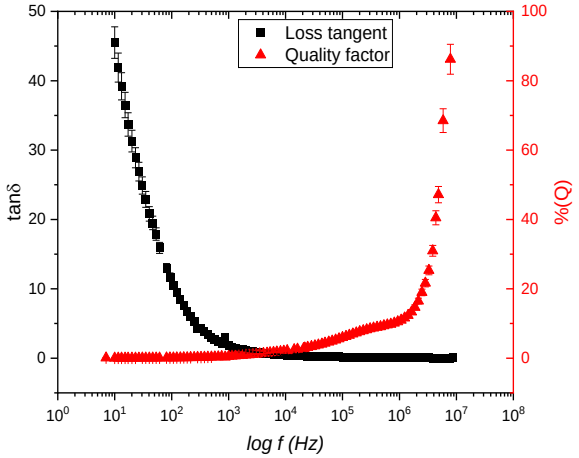

Figure 7: Dielectric loss factor (tanδ) left and quality factor (Q) right variation with frequency working temperature (298 K).

The Nyquist and Cole–Cole plots illustrating the complex components of impedance and dielectric constant are presented in figure 8. The diagram exhibits a semicircular arcs configuration that intersects the x-axis at the points (z'_{∞}, z''_0 and ε'_{∞}, ε'_0) respectively. The spectra arcs in the Nyquist plot (where z' is plotted against z") and as peaks in the Cole-Cole plot (where ε' is plotted against ε") with frequency as running factor *(Cole et al, 2023; Mei et al, 2018).*

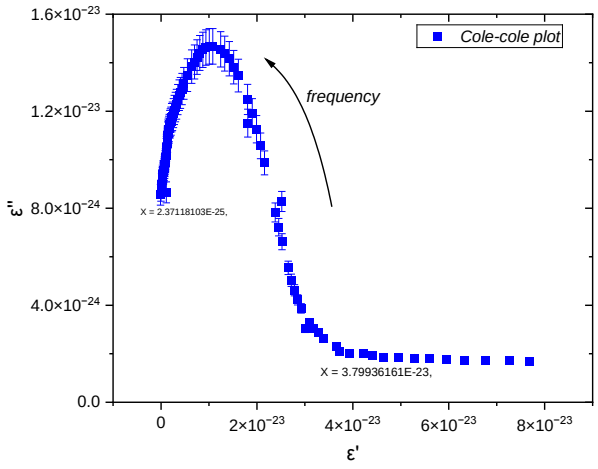

Figure 8 Cole Cole plot for complex dielectric components showing semi-arc pattern**.**

Dielectric Modulus

The dynamic behavior of electrical transport phenomena such as hopping rate of charge carrier, space charge relaxation phenomena, conductivity relaxation mechanism is usually evaluated by complex electrical modulus. Dielectric relaxation, a process characterized by the time-dependent response of a material's polarization to an external electric field, provides insight into the molecular dynamics and structural characteristics of materials *(Natalino et al, 2023)*. Basically, dielectric modulus M*is the reciprocal of dielectric constant ($^1/_{\varepsilon^*}$) and can be represented as complex quantity $M^* = M' + jM$"where M and M* are the real and imaginary parts of the electric modulus.

the experimental data of the imaginary part of the electric modulus was fitted by using Bergmann modified equations to the empirical Kohlrausch, Williams and Watts (KWW) function Equation .

Modified KWW function has been used to fit the M data in order to reduce the number of adjustable parameters and extract the stretched coefficient *(β)*. Relaxation time (τ) can be estimated from the peak maximal frequency (f_{max}) though the relation $\tau = {}^1/_{2\pi f_{max}}$

$$M'' = \frac{M''_{max}}{(1-\beta)+\frac{\beta}{1+\beta}\left[\beta\left(\frac{f_{max}}{f}\right)+\left(\frac{f}{f_{max}}\right)^{\beta}\right]} \qquad \textbf{Equation 9}$$

The occurrence of dielectric loss can be explained as follows: at lowest values of frequency, polarization follows the alternating field applied and polarization contribution is maximal and dielectric loss is neglected. A lag in the dielectric polarization may be noticed concerning the applied alternating electric field which could be caused by the presence of imperfections and impurities in the sample. At the highest frequencies, the field alternates rapidly resulting in slow polarization processes, thus decreasing the dielectric permittivity value. The highest value was observed at low frequency, confirming the contribution of all the polarization effects and suggesting the appearance of ionic conductivity. The dielectric loss in the system mainly originates due to the hopping of localized charge carriers and the creation of defect-induced dipoles. In the low frequency, charge carriers' hopping contributes mainly to high dielectric loss. On the other hand, in the high frequency range, conductive grains are dominant. Therefore, a small amount of energy is required for the exchange of charge carriers over sites which could result in the small value of energy loss *(Natalino et al, 2023).*

The measured values of impedance (Z*) and absolute permittivity (ε*) for EYP sample are plotted against frequency. The variation of both values shows frequency dependence. The complex data was transformed into real and imaginary components, shows the variation of real relative permittivity ε' and imaginary dielectric loss ε" parts of complex dielectric permittivity with frequency. The complex impedance components (real (z') and imaginary(z") are plotted against frequency in in figure 9

The data of Cole-Cole and Nyquist plots are fitted using Simpkin 7.0 software to identify the equivalent circuit model

and describe the electrical response of the system in Figure 8,9 respectively. The frequency dependence of the angle phase (θ) of the complex impedance was evaluated by plotting Bode plot to determine the different contributions in the conduction process.

To investigate the dynamic of charge carrier transport mechanism within the sample, electrical conductivity and electric modulus were investigated. The total conductivity could be considered a summation of both dc and ac components. The conductivity behavior in response of YEP sample is displayed in . Fitting of modified KWW function to imaginary dielectric modulus data measured of the YEP at 298 K sample is illustrated in **Error! Reference source not found.**. The maximal frequency, relaxation time and the stretched coefficient *(β)* was reduced.

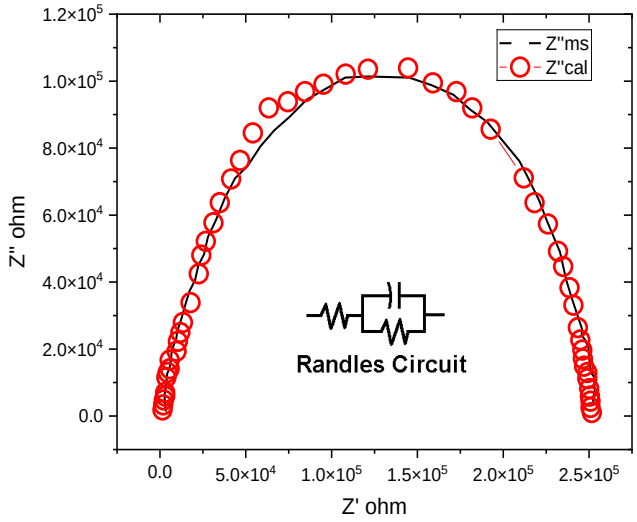

Figure **9** Nyquist plot with fitted curve by Z view software showing equivalent circuit model showing semi-arc pattern

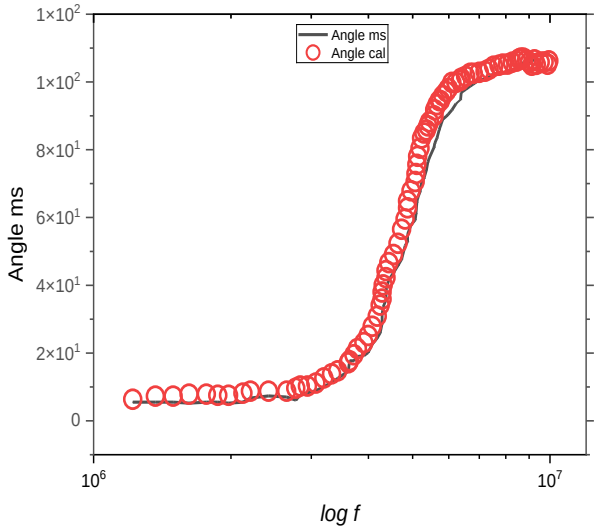

Figure **10** Bode plot with fitted curve by Z view software

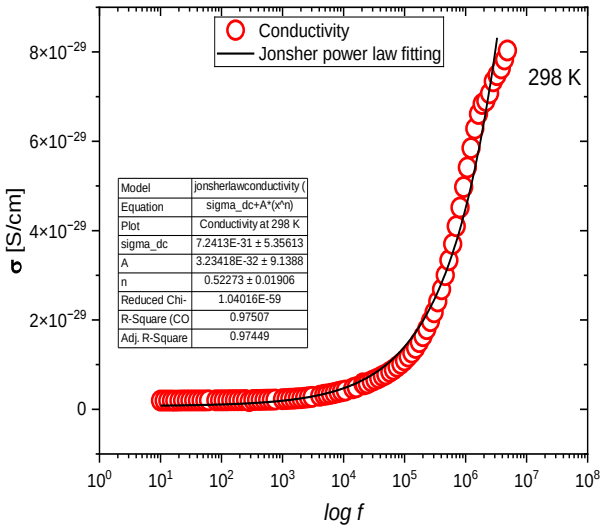

Model	jonsherlawconductivity (
Equation	sigma_dc+A*(x^n)
Plot	Conductivity at 298 K
sigma_dc	7.2413E-31 ± 5.35613
A	3.23418E-32 ± 9.1388
n	0.52273 ± 0.01906
Reduced Chi-	1.04016E-59
R-Square (CO	0.97507
Adj. R-Square	0.97449

Figure **11**: Conductivity variation with applied frequency showing Jonscher fitting curve

The DC conductivity obtained from the power-law fitting (7.24×10^{-31} S/cm) is significantly lower than expected based on the Nyquist plot. This discrepancy may arise from the limited frequency range used in the fitting, which fails to adequately capture the low-frequency plateau required for accurate extraction of DC. Moreover, electrode polarization and interfacial effects at low frequencies may have affected the fitting results, leading to an underestimation of the true DC conductivity. In contrast, the Nyquist plot offers a more direct representation of low-frequency resistive behavior, indicating a higher effective DC conductivity.

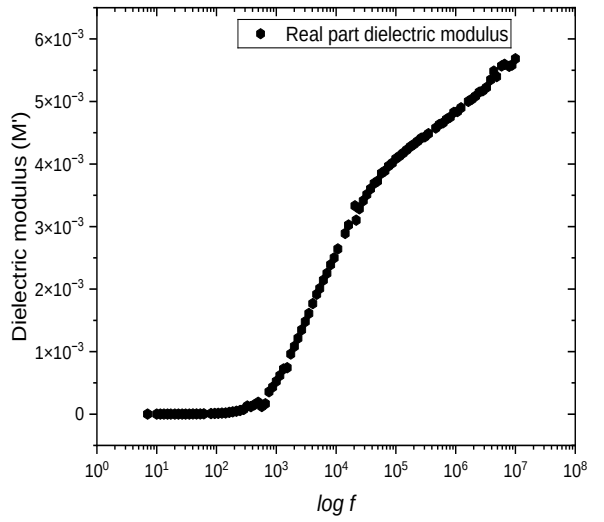

Figure 12: frequency response of real part of dielectric mod

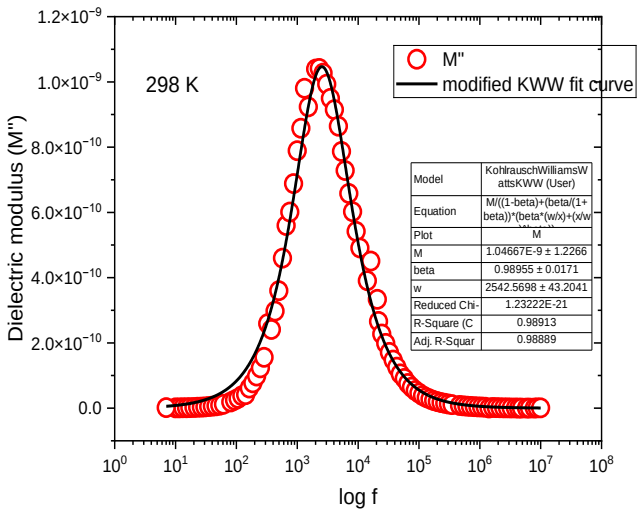

Figure 13 imaginary dielectric modulus variation with frequency showing modified (KWW) fitting curve.

Figure 13 represent a β value of 0.989, which is very close to 1, indicating nearly Debye-type relaxation of the EYP sample. Additionally, discussing the robustness of the β fitting (e.g., confidence interval or model sensitivity) would strengthen the reliability of this analysis.

Discussion

Proteins are polymers composed of polar repeating units of amino acids (a.a.), characterized by the backbone structure (–CO–CR–NH–), and contain neutral, polar, and charged side chains. Due to this structure, proteins can be regarded as polarized materials and are highly sensitive to dielectric analysis. As previously discussed, the ionic state of amino acid zwitterions plays a crucial role in the electrical behavior of EYP, acting as charge carrier dipoles.

Figure 5 presents the measured absolute impedance (Z*) of the EYP sample as a function of the applied frequency. The Z* value decreases with increasing frequency. Both the real (Z') and imaginary (Z") components of the impedance are shown in Figure 7. In the low-frequency range, the magnitude of Z' decreases, which may indicate a higher degree of electric polarization within the sample. At higher frequencies, the Z' value remains relatively constant, suggesting the presence of a relaxation mechanism and a reduction in interfacial barriers.

The imaginary component of impedance, Z", also varies with frequency and reaches a maximum at a specific frequency known as the electrical relaxation frequency (f_max). The peak magnitude of Z" decreases progressively with increasing frequency, indicating space charge accumulation in the system and an associated increase in AC conductivity. This complex impedance behavior suggests that the sample exhibits characteristics typical of semiconducting materials.

The variation of complex dielectric components with frequency is presented in figure 6. Basically, there are four types of frequency dependent polarization mechanisms that involve dielectric behavior of materials: space charge, dipolar polarization, ionic and electronic polarization at lower frequency. The complex dielectric component values increase then decrease with increasing frequency to reach a constant value at a higher frequency range where the contributions from space charge, dipolar and ionic polarization reduce *(Hölzel et al; 1992*).

The first kind of polarization named interfacial or space polarization, and called Maxwell-Wagner effect, appears at low frequencies (<106 Hz). This occurs from the limited displacement of free charges and their accumulation between the different phases of material when those possess distinct permittivity values. This phenomenon is specific for solid and liquid dielectrics, especially with non-homogeneous or amorphous structures. The dipole orientation also called Debye polarization implies the orientation of polar molecules under an electric field at higher frequency (10^6 to 10^{10} Hz). This type of polarization is mainly due to the rotation of amino acids, rotation of charged side groups of proteins, and the relaxation of water interacting with proteins.

Such molecules act as electric dipoles and usually have a permittivity value of 4 or 5 at low hydration level, and up to 10 at higher hydration level. In addition, the loss values usually obtained are low, in the order of magnitude of 10^{-3} to 10^{-2}, which vary with temperature, relative humidity and frequency. Due to the viscosity of the medium, molecules cannot orientate themselves instantaneously to applied electric field as they are subjected to viscosity or Debye forces. Variations of dipole with frequency are called dispersion *(Hölzel et al; 1992*).

Atomic polarization (or ionic) is a result of the atoms displacement linked via ionic bonds (10^{10} to 10^{13} Hz). Induced dipoles are created by Valence electrons travel around orbits shared with other atoms thus. This induced dipole sticks to the electromagnetic field orientation but also takes into account relaxation dynamics. This kind of polarization is well established within 10^{-13} seconds *(Kiani ,2020)*

Electronic polarization is present in almost all types of dielectric materials (>10^{13} Hz). It occurs within 10^{-15} s. The atomic, as well as electronic polarization, creates dipoles that do not comprise energy loss and disappear as soon as the electric field is removed. The influence electromagnetic field on a protein confirms that they are polar materials with amorphous and crystalline parts). Polarization mechanisms are mainly of dipolar orientation (Debye type). In a frequency range 100 MHz and 1 GHz, molecular chains, as well as amino acids are polarized.

The occurrence of dielectric loss can be explained at the lowest frequency; polarization follows the alternating field applied and polarization contribution is maximal and dielectric loss is neglected. At the highest frequencies, the field alternates rapidly resulting in slow polarization processes, thus decreasing the dielectric permittivity value. The highest value was observed at low frequency, confirming the contribution of all the polarization effects and suggesting the appearance of ionic conductivity. The dielectric loss in the system mainly originates due to the hopping of localized charge carriers and the creation of defect-induced dipoles. In

the low frequency, charge carriers' hopping contributes mainly to high dielectric loss. Besides resistive grain boundaries are more effective at low frequency range. Therefore, higher energy is required for the exchange of charge carriers through the cation-anion-cation (c-a-c interactions) interaction which could result in high dielectric loss. On the other hand, in the high frequency range, conductive grains are dominant. Therefore, a small amount of energy is required for the exchange of charge carriers over sites which could result in a small amount of energy loss *(Natalino,2023).*

A Cole-Cole plot is a graphical way to represent impedance data, plotting the imaginary part of impedance against the real part. This plot helps to understand how different parts of a material contribute to its overall electrical behavior (*Barsoukov et al, 2005).*

This discrepancy can happen because the **Nyquist plot** often represents the combined electrical response of the material, and if the grain boundary contribution is weak or overlaps with the bulk response, it may not resolve into a distinct semicircle. (*Macdonald et al, 1987; Boukamp, 1981).*

Cole-Cole and Nyquist plots of the sample are characterized by the appearance of semi-circular arcs that intersect frequency as x-axis at the points (ε'_∞, ε''_0 andz'_∞,z'_0) respectively. These complex plots could be used to assess the presence of Debye or non-Debye type dielectric relaxation in the system. In Debye type relaxation, the center of the semicircle is located on the real axis, whereas for Non-Debye type relaxation the center lies below the real axis (z' axis).In the current work the semicircles centers locate below the real axis (**Error! Reference source not found.** .Such behavior indicates a deviation from ideal-Debye behavior. This Debye behavior might originate from several factors such as the orientation of interior grain, distribution of the size of the grain, grain boundaries, distribution of atomic defects, and effect of stress-strain (*Cole et al,1941; Mei et al, 2018; Ruiz, 2014).*

Electrical Conductivity Analysis

The total conductivity variation with respect to applied frequency (Figure 11) consists of two regions: a plateau corresponding to the DC conductivity, which is frequency-independent and appears at low frequencies, and the AC conductivity, which is frequency-dependent and dominates at higher frequencies. This frequency dependence of the total conductivity indicates the presence of relaxation phenomena in the system. At low frequencies, grain boundaries act as effective insulators, limiting the hopping frequency of charge carriers; therefore, conductivity remains constant (frequency-independent) in this region. Conversely, at higher frequencies, the increased frequency enhances the hopping rate of charge carriers within the conductive grains, leading to a rise in AC conductivity with increasing frequency of the applied field *(Arikawa, 2005).* From the AC conductivity fitting data, values of the exponent below1 indicate translational motion of charge carriers within the sample. Conversely, when **s** is greater than 1, it suggests that the charge carrier motion is localized. In this case, the value of **s** is approximately 0.52, which implies that the charge carriers exhibit translational motion in the sample *(Inna, 2022).*

The Variation of (dielectric modulus (M' and M") as a function of frequency samples are illustrated in figure 7 and figure 12. There is a clear peak at a particular frequency which may originate due to relaxation behavior called relaxation frequency (*fmax*~2542.57 *Hz*). Relaxation frequency suggests the occurrence of conductive relaxation mechanism of charge carriers in the sample. The curve in figure 13 shows an asymmetric nature with respect to relaxation peak relaxation. the stretched exponential is indicated (β~0.99). the value of (β) defines if the relaxation present in the material is of Debye (= unity) or non-Debye type (less < unity). The behavior of (β) obtained by fitting suggests the presence of non-Debye type relaxation in the material.

At low of frequency, charge carriers can move over long distances that can hop from one site to another, a phenomenon known as hopping. On the other hand, at higher frequency ranges charge carriers are confined to their wells and make only localized motions over a short distance within them. That might be due to the defects or interfacial layers between the grains. Overall, the lower frequency range (left side of the relaxation peak) is the area that indicates the conduction process, while higher frequency range (the right of the relaxation peak) is the relaxation process (Natalino,2023 ;Inna,2022).

Conclusion

The application of impedance spectroscopy to analyze yeast-extracted proteins offers a promising approach to addressing food insufficiency by providing a sustainable protein source. This technique leverages advanced analytical methods to optimize protein extraction and characterization. The findings indicate that impedance spectroscopy can yield valuable insights into the electrical properties of yeast proteins, which may correlate with their nutritional and functional qualities. Further research into the molecular structure of yeast-extracted proteins (YETP) and the development of functional modifications for potential medical applications is recommended to explore the use of yeast as a therapeutic dietary supplement to help combat malnutrition.

Data availability

All data generated or analyzed during this study are included in this published article.

References

Anthony, P., H., Wright, Michael, Bruns, Brian, S., Hartley. Extraction and rapid inactivation of proteins from *Saccharomyces cerevisiae* by trichloroacetic acid precipitation. *Yeast*, 5(1):51–53 (1989). https://doi.org/10.1002/YEA.320050107.

Arikawa, T., Yamashita, K., Hirori, H., Nagai, M., & Tanaka, K. Complex dielectric constant of amino-acid solution revealed by THz time-domain attenuated total-reflection technique. (2005, March 14). https://doi.org/10.1364/OTST.2005.WB6.

Asami K, Hanai T, Koizumi N. Dielectric properties of yeast cells. *J Membrane Biol*. 28(2–3):169–80 (1976). https://doi.org/10.1007/BF01869695.

Barsoukov, E., & Macdonald, J. R. (Eds.). *Impedance Spectroscopy: Theory, Experiment, and Applications*. Wiley-Interscience. West, A. R. *Solid State Chemistry and Its Applications*. Wiley. (2005).

Boukamp, B. A., van Miltenburg, J. C., & Bouwmeester, H. J. M. Interpretation of grain boundary effects in impedance spectroscopy. *Solid State Ionics*, 5(3), 285–291 (1981).

Cole, K. S., & Cole, R. H. Dispersion and absorption in dielectrics I. Alternating current characteristics. *J. Chemistry. Physics.*, 9(4), 341–351 (1941). https://doi.org/10.1063/1.1750906.

Dimopoulos, G., et al. Effect of high pressure on the proteolytic activity and autolysis of *Saccharomyces cerevisiae* suspensions. *Innovative Food Science & Emerging Technologies*, 68 (2021). https://doi.org/10.1016/j.ifset.2021.102636.

Gascoyne, P. R. C., & Vykoukal, J. Dielectrophoresis-based sample handling in general-purpose programmable diagnostic instruments. *Proceedings of the IEEE*, 92(1), 22–42 (2002). https://doi.org/10.1109/JPROC.2003.820537.

Hölzel, R., & Lamprecht, I. Dielectric properties of yeast cells as determined by electrorotation. *Biochimica et Biophysica Acta*, 1104, 195–200 (1992). https://doi.org/10.1016/0005-2736(92)90150-K.

Ibarra, E. O. Food sovereignty as an alternative to reducing the serious hunger problem or food shortage worldwide. *Journal of Quality in Health Care & Economics*, 4(2) (2021). https://doi.org/10.23880/jqhe-16000209.

Inna, V., Simakova, V., Strizhevskaya, N. P., Nosacheva, N. V., Bolotova, M. V., Larina, O. V., & Romanova. Development of technological solutions for creating nutritional support for the body. *Vestnik MGTU*, 25(3):239–247 (2022). https://doi.org/10.21443/1560-9278-2022-25-3-239-247.

Jach, M. E., & Malm, A. *Yarrowia lipolytica* as an alternative and valuable source of nutritional and bioactive compounds for humans. *Molecules*, 27(7) (2022). https://doi.org/10.3390/molecules27072300.

Kao, K. C. *Dielectric Phenomena in Solids*. Elsevier Academic Press (2004).

Kiani, M., Du, N., Vogel, M., Raff, J., et al. Disturbing-free determination of yeast concentration in DI water and in glucose using impedance biochips. *Biosensors* (2020, Jan 19).

Kotnik, T., et al. Electroporation-based applications in biotechnology. *Trends in Biotechnology*, 33(8), 480–488 (2015). https://doi.org/10.1016/j.tibtech.2015.06.002.

Chein -Hui Ma. et al. The selfish yeast plasmid exploits a SWI/SNF-type chromatin remodeling complex for hitchhiking on chromosomes and ensuring high-fidelity propagation. *PLoS Genetics*, 19(10) (2023). https://doi.org/10.1371/journal.pgen.1010986.

Macdonald, J. R. Impedance spectroscopy. *Annals of Biomedical Engineering*, 15(2), 119–129 (1987).

Mei, B. A., Munteshari, O., Lau, J., Dunn, B., & Pilon, L. Physical interpretations of Nyquist plots for EDLC electrodes and devices. *Journal of Physical Chemistry C* (2018, Jan 11).

Mirzaei, M., et al. Characterization of yeast protein enzymatic hydrolysis and autolysis in *Saccharomyces cerevisiae* and *Kluyveromyces marxianus*. *Journal of Food Biosciences and Technology*, 5(2), 19–30 (2018).

Natalino, M., & Fumasoni, M. Experimental approaches to study evolutionary cell biology using yeasts. *Yeast*, 40, 123–133 (2023). https://doi.org/10.1002/yea.3848.

NDCs FF. Improving physical and economic access to healthy and sustainable foods – Food Forward NDCs. *Food Forward NDCs* (2024). https://foodforwardndcs.panda.org/food-environment/improving-physical-and-economic-access-to-healthy-and-sustainable-foods/

Olagunju, A. Forest restoration at risk from seed shortage. *Nature Africa* (2023). https://doi.org/10.1038/d44148-023-003257.

Ozols, J. Amino acid analysis. (1990). https://doi.org/10.1016/0076-6879(90)82046-5.

Ruan, C., & Zeng, K. Monitoring of cell viability and proliferation using impedance-based microfluidic chip. *Biosensors and Bioelectronics*, 49, 193–199 (2013). https://doi.org/10.1016/j.bios.2013.05.013.

Ruiz, G. A., Zamora, M. L., & Felice, C. J. Isoconductivity method to study adhesion of yeast cells to gold electrode. *Journal of Electrical Bioimpedance*, 5(1):40–47 (2014). https://doi.org/10.5617/jeb.809.

Stam, J. C., et al. MAP kinase pathways in the yeast *Saccharomyces cerevisiae*. *Microbiology and Molecular Biology Reviews*, 62(4), 554–560 (1998).

Vanderwaeren, L., Dok, R., Voordeckers, K., Nuyts, S., & Verstrepen, K. J. *Saccharomyces cerevisiae* as a model system for eukaryotic cell biology, from cell cycle control to DNA damage response. *Int J Mol Sci.*, 23(19), 11665 (2022). https://doi.org/10.3390/ijms231911665.

Ziso, D., Chun, O. K., & Puglisi, M. J. Increasing access to healthy foods through improving food environment: A review of mixed methods intervention studies with residents of low-income communities. *Nutrients*, 14(11), 2278 (2023). https://doi.org/10.3390/nu14112278.